NUMERICAL MODELING STUDY FOR FLOW PATTERN CHANGES INDUCED BY SINGLE GROYNE

Jungseok Ho[1], Hong Koo Yeo[2], Julie Coonrod[3], and Won-Sik Ahn[4]

[1]Research Assistant Professor, Dept. of Civil Engineering, University of New Mexico, Albuquerque, NM, USA.; PH (505) 573-5079; FAX (505) 277-1988; email: jayho@unm.edu
[2]Senior Researcher, Water Resources Research Department, Korea Institute of Construction Technology, Korea; PH (505) 573-5079; FAX (031) 910-0569; email: yeo917@kict.re.kr
[3]Assosiate Professor, Dept. of Civil Engineering, University of New Mexico, Albuquerque, NM, USA.; PH (505) 277-3233; FAX (505) 277-1988; email: jcoonrod@unm.edu
[4]Professor, Department of Civil Engineering, University of Suwon, Korea; PH (031) 220-2314; FAX (031) 220-2522; email: wsan@suwon.ac.kr

ABSTRACT

Numerical modeling for single groyne in a rectangular section flume was developed to investigate flow pattern changes and to find the best performing installation interval. A three-dimensional computational fluid dynamics model was built to simulate the flow properties near the groyne including the groyne tip velocity and the flow separation length. To evaluate hydraulic influences on the tip velocity and the separation length, four different ratios of groyne length to channel width and five different porous groynes were simulated over varied approach velocity in this study. Permeability of the groyne was reproduced by changing the gap between the cylinders. The approach water depths and the approach velocity acquired from the physical model were treated as the boundary conditions for the numerical model. Computed groyne tip velocity, the separation length, and two-dimensional velocity vectors were compared with the physical model measurements for validation of the numerical model. The numerical model computations showed very positive agreement with the physical model measurements. Relative error analysis showed that the numerical model agreed within 5 % of the physical model for up to 40 % groyne permeabilities. The relationship of the ratio of the computed separation length to groyne length with Froude number was presented and compared with the empirical equation suggested from the physical model. It was found that the numerical model can complement the physical model. The validated numerical model will be used to investigate the effects of the groyne installation angle, series of groynes, and curved channel application for future studies.

KEYWORDS: groyne, recirculation, velocity distribution, numerical models, computational fluid dynamics technique

INTRODUCTION

River groynes are one of the most generally used hydraulic structures to protect against river morphologic instability including channel bank erosion and to improve river ecosystem health. The groyne structure is commonly classified according to permeability of water through the groyne and allocation of the structure along the channel. For practical application and installation of groyne, Yeo et. al. (2005) completed groyne physical model tests with various permeabilities, groyne approach velocities, and groyne lengths. They built a single

groyne in a rectangular sectional flume and tested flow patterns near the groyne for sixty-nine different tasks. The tip velocity of groyne and the two-dimensional velocity field were measured using Acoustic Doppler Velocimeter (ADV) and Large Scale Particle Image Velocimeter (LSPIV) technique. Dimensional analysis for the ratio of the tip velocity to the approach velocity and the ratio of the separation length to groyne length were accomplished to evaluate influencing factors for determining groyne installation interval. Based on the dimensional analysis, Yeo et. al. (2005) suggested an empirical equation describing the relationship between the ratio of the separation length to groyne length and Froude number. The empirical equation showed very good agreement with previous study results including those of Seed (1997) and Ettema and Muste (2004).

In this study, a numerical model was developed to complement the physical model of Yeo et. al. (2005). A three-dimensional Computational Fluid Dynamics (CFD) model of the groyne at the rectangular flume used in the physical model was built and flow patterns around the groyne were simulated. After validation with the physical model measurements, the numerical model can be substituted for the physical model leading to cost and time savings in future groyne system designs.

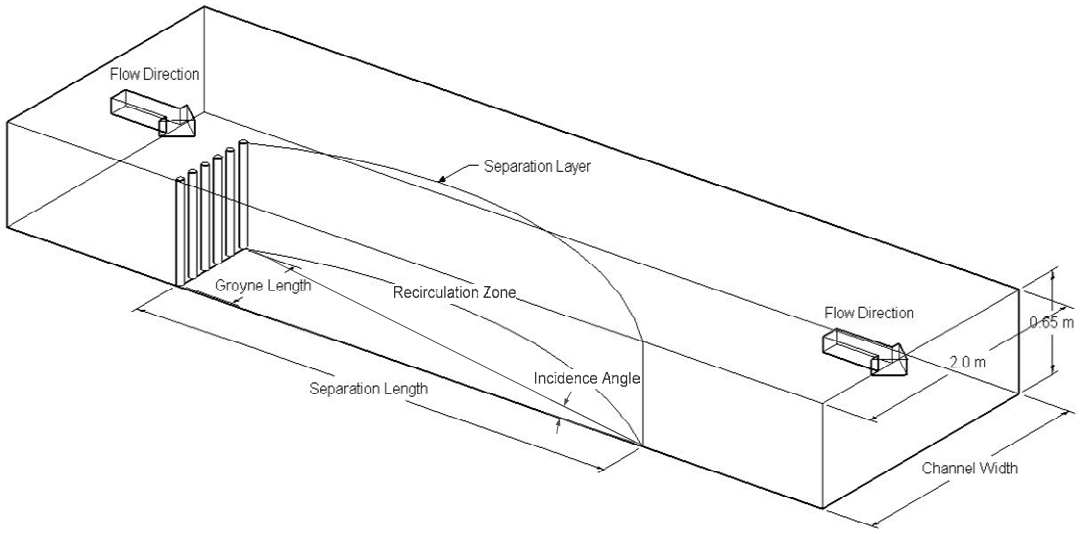

Figure 1 Single groyne model in experimental flume.

MODELING APPROACH

The physical model of the groyne at the rectangular flume and a schematic sketch of the flow pattern is shown in Figure 1. A recirculation zone is produced behind the groyne since the groyne constricts flow, developing an eddy flow with the main current. A separation layer represents the boundary of the recirculation zone, while the distance between the groyne and end of the separation layer is defined as the separation length. The purpose of this study was to develop a numerical model to complement the physical model for the groyne hydraulic experiments. Using the numerical model, flow pattern changes induced by the single groyne at the rectangular section channel were simulated. Hydraulic properties of the groyne tip velocity, the separation length, and two-dimensional velocity vector within the recirculation zone were simulated and reproduced using the numerical model. Various lengths and permeabilities of groyne and approach velocities were tested in this numerical model for the best performing installation interval of a single groyne.

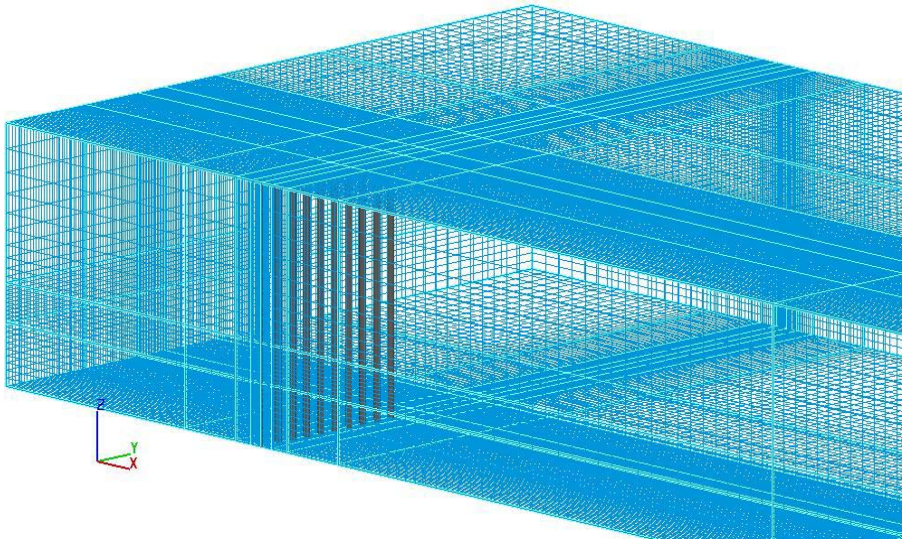

Figure 2 Finite volume mesh of the groyne model.

Four numerical model scenarios were simulated with the groyne installation ratio of groyne length to channel width: 0.10, 0.15, 0.20, and 0.25. Five porosity values of the groyne were tested: 0 % (impermeable), 20 %, 40 %, 60 %, and 80 %. The approach velocity varied from 0.25 m/s to 0.47 m/s, resulting in a total of sixty-nine simulation scenarios, similar to the physical model experiments. For the numerical model boundary conditions, the approach water depths and velocity measured from the physical model were used. The computed tip velocity and the separation length were compared with the physical model measurements for validation of the numerical model.

NUMERICAL MODEL

Steady state incompressible flow conditions with viscosity and inertia effects are generally considered in hydraulic numerical modeling, and the Navier-Stokes equation has been well adapted to solve the governing equation. The Navier-Stokes equation is an incompressible form of the conservation of mass and momentum equations, and is composed of non-linear advection, rate of change, diffusion, and source term in the partial differential equation. The mass and momentum equations coupled via velocity can be used to derive an equation for the pressure term. When turbulent flow phenomenon should be considered in the Navier-Stokes equation, the computation becomes more complex. In this approach, the Reynolds-Averaged Navier-Stokes (RANS) equations are commonly used. It is a modified form of the Navier-Stokes equation including the Reynolds stress term, which approximates the random turbulent fluctuations by statistics.

In this study, the commercially available Computational Fluid Dynamics (CFD) program Flow-3D, developed by Flow Sciences, was used for the numerical modeling. This computer program solves the RANS equations by the finite volume formulation obtained from a staggered finite difference grid. For each cell, average values for the flow parameters, pressure and velocity, are computed at discrete times. The new velocity in each cell is estimated from the coupled momentum and continuity equation using the initial conditions or previous time step values. The pressure term is solved and adjusted using the computed velocity to satisfy the continuity equation.

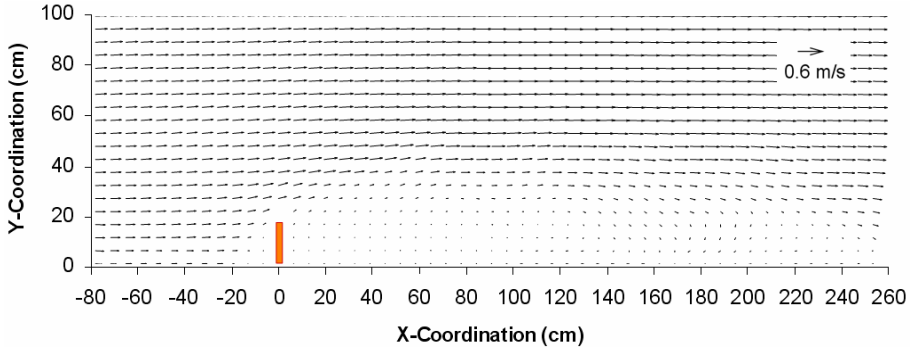

(a) Measurements

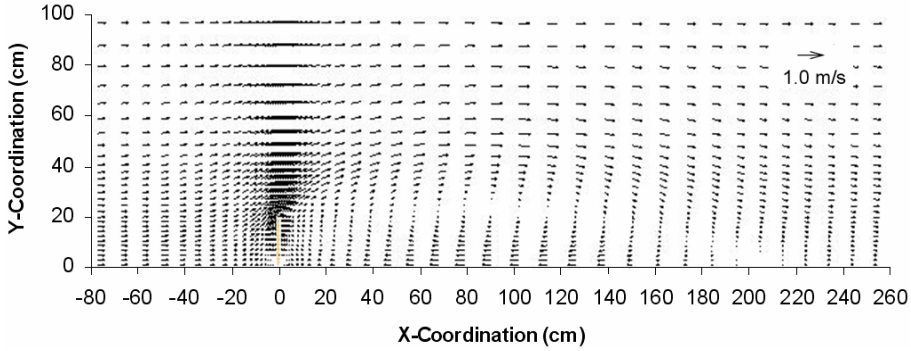

(b) Computations

Figure 3 Velocity vector comparison (groyne l = 0.20 m, P = 0 %, and V_{app} = 0.25 m/s).

With the computed new velocity and pressure, remaining variables are estimated including density advection and diffusion, turbulent transport, and wall function evaluation. Five turbulence models are available in this CFD program: Prandtl mixing length, the one-equation turbulence energy, the two-equation κ-ε equation, the renormalization-group, and the large eddy simulation.

For tracking of the fluid interfaces, the Volume Of Fluid (VOF) method was used. With the VOF method, grid cells are classified as empty, full, or partially filled with fluid. Cells are assigned the fluid fraction varying from zero to one, depending on quantity of fluid. Along the fraction cells, advection of fluid changing and the given boundary conditions at the free surface (zero fraction cells) maintain the sharp interface. The free surface slope of a partially filled cell is computed by free surface angle and location of the surrounding cells, and then it is defined by a series of connected chords in the two-dimensional model or by connected planes in the three-dimensional model. These fractions are embedded into all terms of the RANS equations. For mesh geometry on the finite control volume, the Fractional Area/Volume Obstacle Representation (FAVOR) method, developed by Hirt and Sicilian (1985) was used. The FAVOR method is a porosity technique, which defines an obstacle in a cell with a porosity value between zero and one as the obstacle fills in the cell. Geometries are embedded in the mesh by setting the area fractions on the cell faces along with the volume fraction open to flow (Hirt, 1992). It makes independent geometry specifications on the grid, and as a result, complex obstacles can be generated. Each obstacle within a grid is specified as a volume fraction (porosity) to represent a solid condition such as completely solid, part solid and fluid, completely fluid, part fluid, or completely empty.

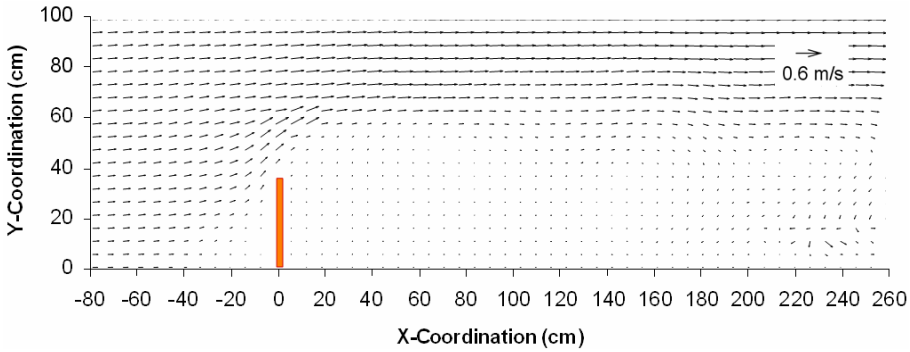

(b) Measurements

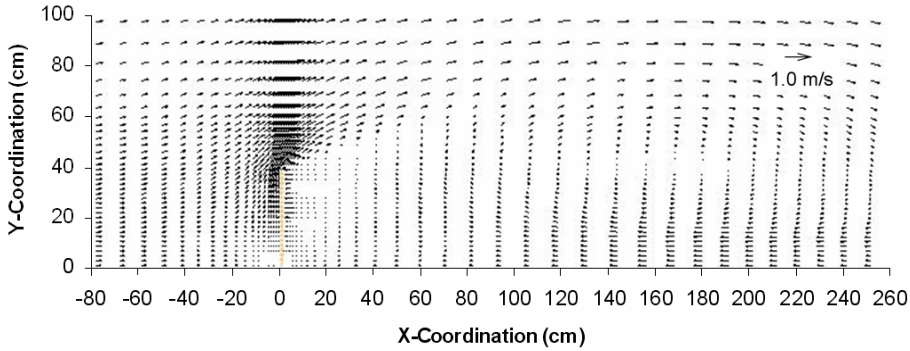

(b) Computations

Figure 4 Velocity vector comparison (groyne l = 0.4 m, P = 0 %, and V_{app} = 0.25 m/s).

MODEL IMPLEMENTATION

Various sizes of the hexagon grid cells were meshed ranging from 0.14 cm^3 to 35.0 cm^3 in volume. This grid was modified to a finer grid after the preliminary computation reached steady state, and then the following computations were initialized on the modified finer grid at the sequential re-run of the model. To model the groyne, a series of solid cylinders with 2 cm diameter was meshed on 200 cm wide (y-coordination) and 65 cm deep (z-coordination) of rectangular sectional grid domain. The length of the mesh (x-coordination) was varied depending on the flow separation length caused from the recirculation zone induced by the groyne to save computational time and memory. Four different lengths of the groyne, 20.0, 30.0, 40.0, and 50.0 cm were tested based on different groyne installation ratios of groyne length to channel width. Permeability of the groyne was reproduced by changing the gap between the cylinders. In the case of the 30 cm groyne length with 20 % permeability, twelve cylinders were composed with 2.545 cm of gap. For the 60 % permeability, six cylinders and 5.6 cm of gap were used. Figure 2 shows the finite volume mesh of the 50 cm groyne length with 60 % of permeability scenario. Ten cylinders were built with 5.333 cm of gap between each other.

For the upstream boundary condition, the stagnation pressure value was used in this model. The stagnation pressure, $P + \rho V^2/2$, boundary condition assumed that the fluid next to the boundary is stagnant at the specified pressure value which is an approximation to a large reservoir of fluid outside the mesh domain (Flow Sciences, 2003). In this model, a fluid height was used for the stagnation pressure boundary condition of the inflow to the domain. The upstream boundary conditions were applied varying from 15.3 cm to 25.1 cm depending on the approach water depth and velocity.

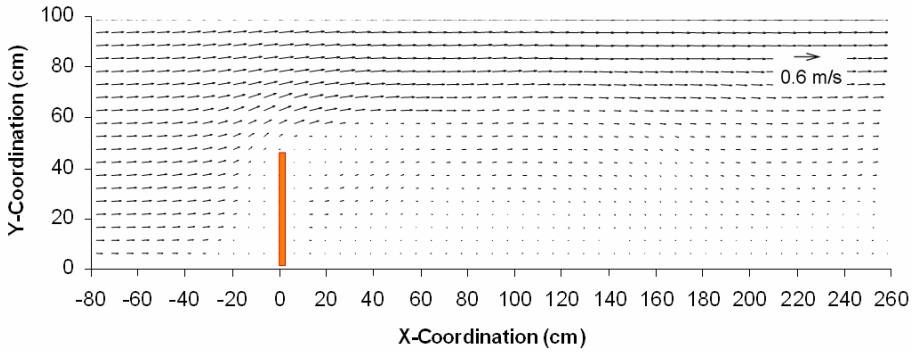

(a) Measurements

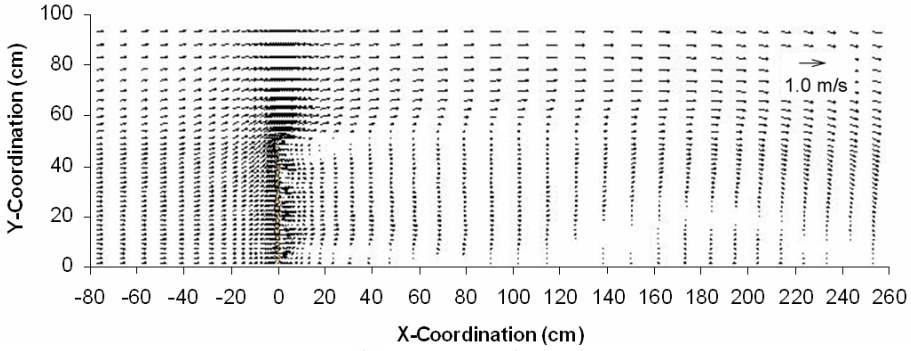

(b) Computations

Figure 5 Velocity vector comparison (groyne l = 0.5 m, P = 20 %, and V_{app} = 0.30 m/s).

On the other hand, the continuative boundary condition, which consists of zero normal derivatives at the boundary for a smooth continuative flow through the boundary, was adopted as the downstream boundary condition to evaluate the outflow rate with the physical model measurements. Atmosphere pressure was set at the top of the mesh, and no slip wall boundary condition, having zero tangential and normal velocities, was applied at the bottom and sidewall of the domain. The z-coordinate limited fluid region was initialized to the approach water depth, while the x-coordinate initial velocity was initialized to the approach velocity. These initial conditions allow for a fast numerical convergence. For the turbulence model, the two-equation κ-ε equation was adopted, and the successive over relaxation method was used for the pressure convergence.

RESULTS

The tip velocity, the separation length, and the velocity vectors were computed with various groyne installation ratios of groyne length to channel width, permeabilities, and approach velocities. Computations of the two-dimensional velocity vectors near the groyne were compared with the physical model measurements. Computed tip velocity and separation length were normalized and analyzed in a non-dimensional form.

Figure 3 shows the velocity vectors for 0.2 m long impermeability groyne with 0.4 m/s of the approach velocity. The numerical model (Figure 3 (b)) computed a 2.24 m separation length and 5.10° incidence angle, while 2.35 m separation length and 4.86° incidence angle were obtained from the physical model measurements (Figure 3 (a)). Recirculation zones rotating clockwise were found in both models.

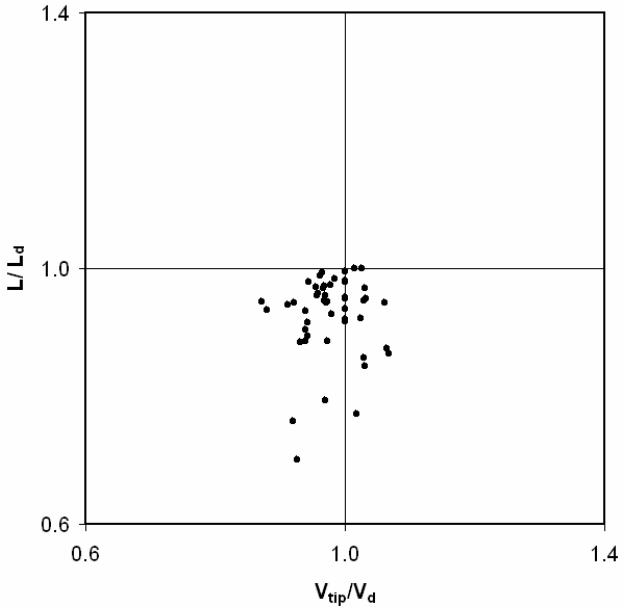

Figure 6 Normalized separation length and tip velocity.

In the numerical model, the center of the recirculation zone separated from the channel side wall, unlike the results of the physical model. Also, the numerical simulations produced high negative velocities reversing against the main current. Less dense and multiple eddies composed the recirculation zone in the physical model as compared to the numerical model simulation.

A high intensive vortex was generated at the tip of the groyne in both models. Velocity increased along the increasing water depth from the tip to the downstream of the groyne in the middle of the channel. Slightly higher tip velocity (0.34 m/s) was computed than was measured (0.31 m/s). The tip velocity of the groyne was obtained at the middle layer (60 % of the water depth).

Velocity vectors near the 0.4 m long impermeable groyne with 0.25 m/s approach velocities are shown in Figure 4. The recirculation zone is wider and longer than the 0.2 m long groyne scenario. The tip velocity was measured at 0.39 m/s and the separation length was observed to be 4.90 m (4.67° incidence angle). These flow patterns were reproduced by the numerical model as shown in Figure 4 (b). A 0.35 m/s tip velocity and 4.68 m separation length (4.89 ° incidence angle) were computed. In most cases, the tip velocity was approximately 1.5 times higher than the approach velocity.

For the impermeable groyne scenarios, direct proportion relationship between the separation length and the groyne length was obvious. However, the direct proportion relationship was diminished with increasing permeability of the groyne. Velocity vectors near the groyne of 0.5 m length 20 % permeability with 0.3 m/s of the approach velocity are shown in Figure 5. The separation layer extended 4.80 m downstream (5.95° incidence angle), and 0.42 m/s tip velocity was measured in the physical model (Figure 5 (a)). Indistinct flow patterns of the recirculation zone were found compared with the impermeable groyne scenarios. The numerical model provided explicit flow patterns of the recirculation zone including the gaps between the cylinders used for the groyne permeability. A 0.38 m/s tip velocity was computed and 0.25 m/s average velocity was obtained at the gap of the cylinder. At the recirculation zone, 4.61 m separation length and 6.19° incidence angle were computed.

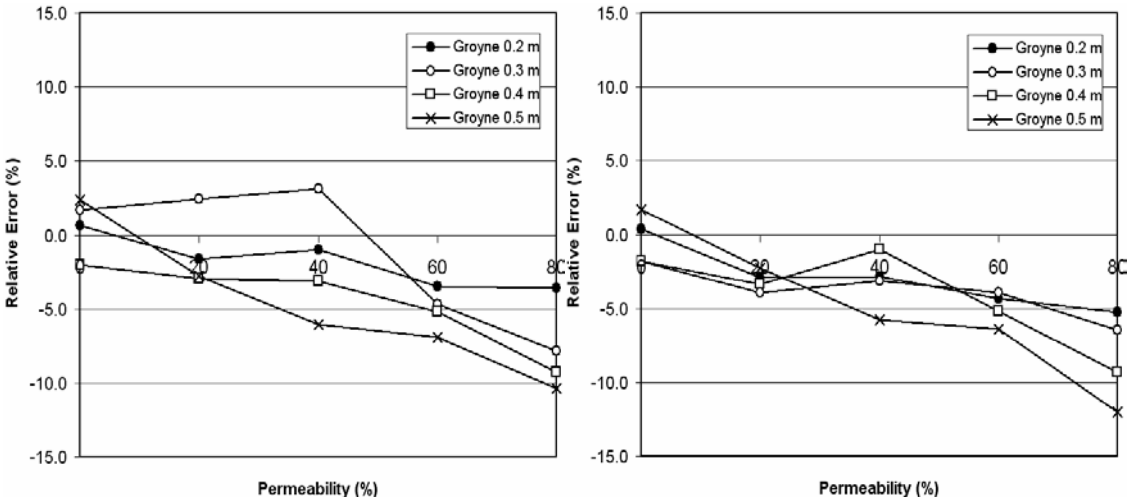

(a) Approach velocity 0.25 m/s (b) Approach velocity 0.40 m/s

Figure 7 Tip velocity relative error versus groyne permeability.

The computed separation length (L) and the groyne tip velocity (V_{tip}) were normalized with respect to the design separation length (L_d) and the design tip velocity (V_d), respectively, to provide an analysis in non-dimensional form. Figure 6 shows the normalized separation length against the normalized tip velocity. The measurements from the physical model test were used as the design values. The normalized values are distributed under the separation length standard (L/L_d = 1.0) and middle of the tip velocity standard (V_{tip}/V_d = 1.0). From an analysis of the normalization, it was found that most of the computed separation lengths were lower than the physical model measurements, while the tip velocities were simulated adequately.

The relative error of the tip velocity at the groyne permeability was calculated to analyze the numerical model agreement with the physical model. Figure 7 shows the tip velocity relative error at the groyne permeability for the groyne length. The relative error is defined as $(V_c - V_m)/V_m \times 100$, where V_c is the computed tip velocity and V_m is the measured tip velocity. The relative error analysis shows that the numerical model agrees to within 5 % of the physical model for groyne permeabilities up to 40 %, except for the scenarios of 0.25 groyne installation ratio of groyne length to channel width (0.5 m of groyne length in this model). In both approach velocity scenarios (0.25 m/s and 0.40 m/s), the numerical model shows better agreement at the less permeable and low groyne installation ratio. The high computation difference in the permeable groyne model cases cause from flow disturbance induced by a permeable groyne.

The relationship of the ratio of the computed separation length to groyne length with Froude number was obtained as shown in Figure 8. These computations were compared with the empirical equation (equation 1) suggested from the physical model measurement by Yeo et. al. (2005). Although the separation length ratio was limited only for $0.17 \le Fr \le 0.38$, the numerical model computations agree well with the suggested empirical equation.

$$L^* = 12.616 \times K_\alpha \times K_p \times Fr^{0.0323} \qquad \text{Equation 1}$$

where, $L^* = L/l$, K_α is the coefficient of installation angle, K_p^* = -0.14 × P + 12.066, the coefficient of permeability (0 % < P (permeability) ≤ 80 %).

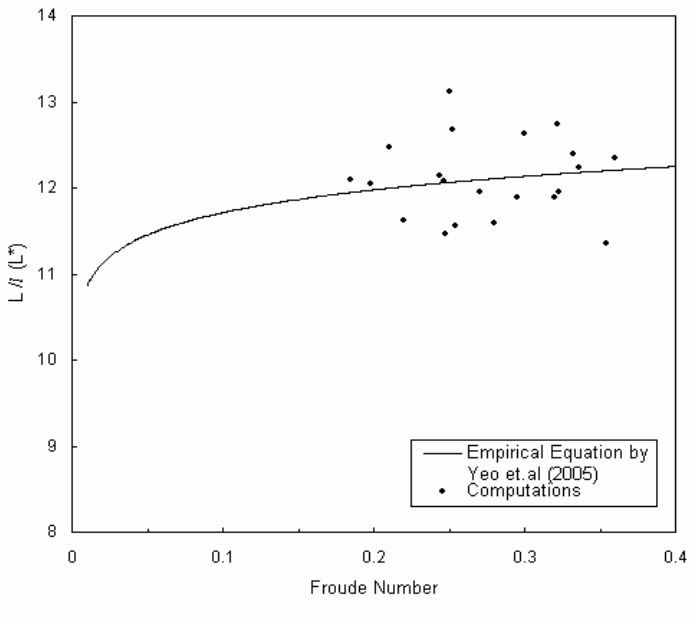

Figure 8 Normalized tip velocity comparison.

Different data probe locations between the physical model and the numerical model are another potential cause of errors. The surface velocity vectors observed in the physical model test were compared with the 10 % average water depth computed values to prevent data discontinuity.

The experimental flume length used in the numerical model may cause the simulation differences between the simulation results and the physical model measurements. The groyne model was built in an approximately 40.0 m long experimental flume and water was supplied over a 1.2 m high weir. Conversely, a 12.0 m long flume was meshed in the numerical model to save computational time and memory. Even though the numerical model uses an average water pressure head and velocity head from the physical model for its upstream boundary condition, differences with the physical model should be expected.

CONCLUSIONS

Flow pattern changes induced by a single groyne in a rectangular channel were numerically simulated using a three-dimensional CFD model. The numerical model was simulated with various groyne installation ratios of groyne length to channel width, groyne permeabilities, and groyne approach velocities. Computations of the tip velocity, the separation length, and the velocity vectors were validated with the physical model measurements completed by Yeo et. al. (2005). The relationship of the ratio of the computed separation length to groyne length with Froude number was presented and compared with the empirical equation suggested from the physical model measurement. The separation length can provide useful information for the groyne installation interval. Groyne permeability had one of the greatest effects on the separation length in this study. Separation length was simulated at 12.5, 5.7, and 1.8 times longer than groyne length for 0 % (impermeable), 20 %, and 80 % permeabilities, respectively. It is found that the groyne numerical model can be substituted for the physical model and leads to cost and time savings in future groyne system designs. Most of the computed separation lengths were lower than the physical model measurements, while the tip velocities were simulated adequately. In addition, the relative error analysis showed that the numerical model agreed within 5 % of the physical model for

up to 40 % of groyne permeability. The numerical model provided reliable computations in the case of the less permeable groyne and the low groyne installation ratio. The validated numerical model will be used to investigate the effects of the groyne installation angle, series of groyne, and curved channel application studies.

ACKNOWLEDGEMENTS

The writers would like to thank Joon Gu Kang and Sung Jung Kim for the physical model tests and measurements collection at the Water Resources Research Department, Korea Institute of Construction Technology.

REFERENCES

1. Ettema, R. and Muste, M. (2004). "Scale effects in flume experiments on flow around a spur dike in flatbed channel." *Journal of Hydraulic Engineering*, ASCE, 130(7), 635-646.
2. Flow-3D user manual; excellence in flow modeling software, v 8.2. (2003). Flow Science, Inc., Santa Fe, NM.
3. Hirt, C. W., and Sicilian, J. K. (1985). "A porosity techniques for the definition of obstacles in rectangular cell meshes." *Proc., 4th Int. Conf. Ship Hydro.*, National Academy of Science, Washington, D.C., 1-19.
4. Hirt, C. W. (1992). "Volume-fraction techniques: powerful tools for flow modeling." *Flow Sciences Report FSI 92-00-02*, Flow Science, Inc., Santa Fe, NM.
5. Seed, D. J. (1997). "Guidelines on the geometry of groynes for river training." *Report SR 493*, HR Wallingford, England.
6. Yeo, H. K., Kang, J. G., and Kim, S. J., (2005). "An experimental study on tip velocity and downstream recirculation zone of single groynes of permeability change." *Korean Journal of Civil Engineering*, Korean Society of Civil Engineers, 9(1), 29-38.